## ORIGINAL RESEARCH



# Cigarette filters: a benchmarking investigation of thermal and chemical attributes

Eric Wilkinson · Margaret Stack · Eunha Hoh · Sarah Poletti · Natalie Mladenov · George Youssef

Received: 28 June 2024 / Accepted: 28 September 2024 / Published online: 4 October 2024 © The Author(s), under exclusive licence to Springer Nature B.V. 2024

Abstract Cellulose acetate (CA) has been extensively studied with minimal regard to end-of-life analysis. Cigarette filters predominantly comprise CA fibers and chemical additives for filtration and manufacturing, altering their physicochemical and thermal properties and influencing their interactions with the environment upon disposal. This research established and employed multifaceted analyses to determine the physicochemical and thermal properties of cellulose acetate sourced from unsmoked cigarette filters and pristine CA powder, including Fourier transform

**Supplementary Information** The online version contains supplementary material available at https://doi.org/10.1007/s10570-024-06202-2.

E. Wilkinson · G. Youssef (⋈) Experimental Mechanics Laboratory, Mechanical Engineering Department, San Diego State University, 5500 Campanile Drive, San Diego, CA 92182, USA e-mail: gyoussef@sdsu.edu

M. Stack · E. Hoh School of Public Health, San Diego State University, 5500 Campanile Drive, San Diego, CA 92182, USA

M. Stack San Diego State University Research Foundation, San Diego, CA 92182, USA

S. Poletti · N. Mladenov Water Innovation and Reuse Laboratory, Department of Civil, Construction and Environmental Engineering, San Diego State University, 5500 Campanile Drive, San Diego, CA 92182, USA infrared spectroscopy (FTIR), optical and electron microscopy, thermogravimetric analysis (TGA), and differential scanning calorimetry (DSC). FTIR analysis ascertained the structure of CA by resolving spectral peaks while pointing out the effects of additives, processing conditions, and the degree of substitution. An increase in the latter indicates reduced biodegradability and potentially longer persistence after disposal. The morphology was examined using electron and optical microscopies, revealing insights into FTIR results. TGA elucidated the decomposition response, evidencing moisture and volatile retention in the CA fibers extracted from unsmoked cigarette filters, suggesting unique decomposition behavior due to the reactivity of the additives with the surrounding environment. The thermal decomposition of unsmoked cigarette filters is insensitive to inter- and intra-filter variability. DSC analysis identified the thermal transitions of the CA fibers and powder, accentuating the effects of morphology, entanglements, and plasticizers on the structural stability of cellulose acetate. Our research establishes a baseline characterization of cigarette filters, laying the scientific foundations for further investigations into this pervasive pollutant.

**Keywords** Cigarette filters · Cellulose acetate · Infrared spectroscopy · Thermal gravimetric analysis · Differential scanning calorimetry · Activation energy



## Introduction

A prominent environmental challenge nowadays is the proliferation and endurance of microplastics in nature upon disposal, with cigarette filters (predominately comprising cellulose acetate, CA) at the forefront as the most littered artifact worldwide (Vanapalli et al. 2023). Despite the natural source of cellulose acetate, the processing conditions and manufacturing parameters play an active role in its resilience after disposal. The slow decomposition of processed cellulose acetate is further exaggerated by chemical additives that stabilize the thermal and mechanical behavior during manufacturing and forecasted deployment in real-life applications, e.g., cigarette filters. The relatively small size of the cigarette filters and the progressive mechanical breakdown process (slower than desired or anticipated) facilitate the pollution of waterways and potentially pose significant hazards to living beings feeding off these water sources (Gola et al. 2021). Therefore, the primary motivation of the research is to explore the thermal and physicochemical properties of the ubiquitous cellulose acetate formulation in cigarette filters to potentially reveal the conditions conducive to accelerated decomposition in natural environments.

Cellulose acetate is a very adaptable chemical compound integrated into various applications and has attracted assiduous research that emphasized novel compositions, processes, and applications (Candido et al. 2017; Charvet et al. 2019; Filho et al. 2008; Teixeira et al. 2021; Vinodhini et al. 2017). For example, Charvet et al. (2019) studied manufacturing cellulose acetate using injection molding, reporting a correlation between an increase in impact resistance, the plasticizer weight ratio (wt.%), and the strain hardening behavior. Meireles et al. (2007) studied the synthesis of cellulose acetate from sugarcane bagasse, developing the miscibility characteristics of cellulose acetate/polystyrene blends, and investigating the dependence of the thermal properties on the processing conditions and the presence of modifying chemical additives. Candido et al. (2017) furthered the characterization of cellulose acetate produced from sugarcane bagasse, reporting insensitivity of the thermal properties to the presence of some additives, and a correlation between the thermal properties and some manufacturing parameters, namely solvent evaporation time. Bao et al. (2015) emphasized the characterization of neat and plasticized cellulose acetate, identifying a large miscibility envelope and showing that the relaxation responses of higher wt.% plasticizer blends (≥25 wt.%) obey Vogel-Fulcher-Tammann law. While there is expansive literature on the thermal and physicochemical properties of neat and plasticized cellulose acetate (Bao et al. 2015; Candido et al. 2017; Charvet et al. 2019; Erdmann et al. 2021; Filho et al. 2008; Lucena et al. 2003; Teixeira et al. 2021; Wang et al. 2016), there is a gap in the current understanding of the specific properties of cellulose acetate extracted from off-the-shelf cigarettes, hence the motivation for this research.

Cellulose acetate refers to several acetate esters of cellulose (Fischer et al. 2008), of which diacetate has garnered keen research efforts, being the most common ester, including in manufacturing cigarette filters (Serbruyns et al. 2023). Physicochemical characterization using spectroscopic techniques is imperative to fully explore the chemical structure of cellulose acetate and its derivatives. For example, Dias et al. (1998), Murphy and Pinho (1995), Oldani and Schock (1989), and Toprak et al. (1979) identified multiple characteristic spectral peaks of cellulose acetate (CA) using Fourier transform infrared spectroscopy (FTIR) of CA membranes with specific attention to the effects of water adsorption and absorption. Toprak et al. (1979) identified peaks at 1752 cm<sup>-1</sup> (stretching in the carbonyl group), and 1233 and 1050 cm<sup>-1</sup> (stretching of the C-O bond). Murphy and Pinho (1995), along with Oldani and Schock (1989), independently reported identical spectral peaks at 1744 cm<sup>-1</sup> (stretching in the carbonyl group) and at 1228 and 1044 cm<sup>-1</sup> (stretching of the C-O bond). Dias et al. (1998) also revealed similar spectral peaks at 1740 cm<sup>-1</sup> (stretching in the carbonyl group) and at 1220 and 1040 cm<sup>-1</sup> (stretching of the C-O bond). These studies also discussed the effect of moisture in the CA membranes on the spectral response, denoting spectral peaks at 2945 and 2890 cm<sup>-1</sup> (Murphy and Norberta de Pinho 1995; Oldani and Schock 1989), or 2940 and 2880 cm<sup>-1</sup> (Dias et al. 1998), as -CH stretching and spectral peaks around 3500 to 3100 cm<sup>-1</sup> as -OH stretching (Dias et al. 1998; Murphy and Pinho 1995; Oldani and Schock 1989; Toprak et al. 1979), all of which are in agreement with other independent reports (Filho et al. 2008; Ilharco and Barros 2000). Vinodhini et al. (2017) and Skornyakov and Komar (1998) worked on the FTIR of plasticized



CA, noting shifts in the characteristic peaks as a function of the plasticizer content at low doping levels. Skornyakov and Komar (1998) theorized that the plasticizer content of cellulose acetate might be determined by comparing the relative peak intensities of non-plasticized and plasticized samples. Similarly, Fei et al. (2017) used FTIR analysis to determine the degree of substitution (DS) in CA by comparing the relative peak intensities of the 1750, 1370, and 1240 cm<sup>-1</sup> peaks to that at 1040 cm<sup>-1</sup> by using two baseline adjustments across the valleys between 2000 and 1680 cm<sup>-1</sup> and 1600 and 940 cm<sup>-1</sup>. Degrees of substitution ranging from 1.8 to 3.0 were reported for CA processed by mixing varying ratios of cellulose and cellulose triacetate (DS = 3) and acetalizing cotton-based cellulose using acetic anhydride (Ac<sub>2</sub>O) for varying lengths of time and reaction temperatures (Fei et al. 2017). Despite this large body of research, the physicochemical characterization of CA in cigarette filters remains understudied, which is imperative for the degradation efficacy of CA once the filters are disposed; hence, the current study introduces a baseline FTIR characterization of the plasticized CA in the filters.

Interaction with the surrounding environment implies an intrinsic relationship between the disposed filters and temperature. Much of the research characterizing cellulose acetate using thermogravimetric analysis (TGA) focuses on the effects of plasticization. Quintana et al. (2013) illustrated the change in degradation temperature based on the plasticizer type, emphasizing eco-friendly plasticizers. The degradation temperature (372 °C for neat cellulose acetate) shifted by up to 5 °C lower depending on plasticizer type and content ratio (Quintana et al. 2013). Teixeira et al. (2021) reported on the thermal degradation of CA, noting that the primary degradation occurs between 313 and 394 °C (for neat CA films) and shifts to 217 and 407 °C for plasticized counterparts. In addition, the report also examined the change in the degradation range (332–401 °C) of CA films over time when exposed to environmental elements (Teixeira et al. 2023). Lucena et al. (2003) used TGA to investigate the decomposition of CA as a function of heating rate, ranging between 2.5 and 40 °C/min. They reported a corresponding change in the degradation temperatures from ~340 to 400 °C. Candido et al. (2017) and Meireles et al. (2007) studied the properties of CA produced from sugarcane bagasse, reporting degradation ranges of 200-380 °C and 300-400 °C, respectively, elucidating the interrelationship between the decomposition of CA, the final chemical structure, and the processing conditions. Another aspect of TGA research is decomposition kinetics (a direct method for determining activation energy), initially developed by Flynn and Wall (1966) and Ozawa (2006). Decomposition kinetics leverages the changes in thermal decomposition behavior as a function of heating rate to resolve the activation energy based on Arrhenius processes codified in ASTM E1641-23 (2023). Ferreira et al. (2022) calculated an Arrhenius activation energy of 138 kJ/mol for a pure CA membrane, while Lucena et al. (2003) reported a range of activation energy between 143 and 152 kJ/mol for CA powder. The variation mentioned above in the onset of degradation and activation energy of CA highlights the strong coupling between decomposition, CA formulation, and modifying additives (e.g., plasticizers), motivating the research leading to this report in exploring the thermal decomposition response of cellulose acetate extracted from cigarette filters.

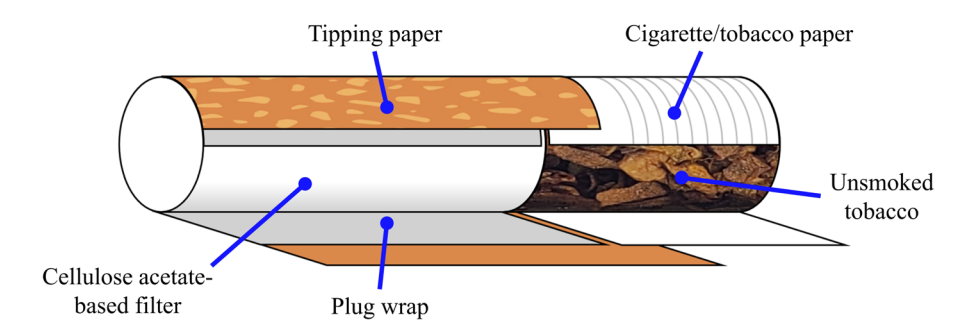
Another aspect of thermal analysis utilizes differential scanning calorimetry (DSC) to elucidate the effect of processing conditions on thermal transition points of cellulose acetate, including glass transition  $(T_g)$  and melting  $(T_m)$  points. The former defines the transition from the brittle (glassy) state to the deformable and malleable (leathery and rubbery) state. At the same time, the latter denotes the phase transition from the solid to the liquid state. The thermal response is imperative for processing CA into the final product, e.g., cigarette filters. Quintana et al. (2013) determined the  $T_g$  of various eco-friendly plasticized cellulose acetate blends, reporting a  $T_g \approx$ 190 °C for neat CA and a  $T_g \approx 109-157$  °C for plasticized blends. Candido et al. (2017) reported  $T_g = 200$ °C for the sugarcane bagasse-based cellulose acetate. Buchanan et al. (1996) investigated the relationship between T<sub>g</sub> and the degree of substitution, showing that the change in glass transition is inversely related to DS (e.g.,  $\rm T_{\rm g}\approx 189~^{\circ}C \rightarrow 209~^{\circ}C$  corresponds to DS =  $2.5 \rightarrow 2.0$ ). Bao et al. (2015) discussed the effect of plasticizer content on the glass transition of CA, where  $T_g \approx 192$  °C for neat CA falls to  $T_g \approx 50$ °C for 50 wt.% plasticizer (diethyl phthalate). Similarly, Erdmann et al. (2021) studied the effects of plasticizers on the T<sub>g</sub> of cellulose acetate, reporting a



 $T_g \approx 197$  °C for neat CA and a shift to  $T_g \approx 76-142$  °C for plasticized CA blends (glycerol triacetate and triethyl citrate ranging from 15 to 40 wt.%). Charvet et al. (2019) reported a  $T_g$  value of 135 °C for 15 wt.% plasticizer blends and a  $T_g$  of 100 °C for 30 wt.% plasticizer blends when characterizing injection molded CA. Wang et al. (2016) reported a  $T_g$  of 202 °C for neat CA,  $T_g \approx 115$  °C for 15 wt.%,  $T_g \approx 108$  °C for 20 wt.%, and  $T_g \approx 99$  °C for 25 wt.% of polyethylene glycol 200 plasticized CA. While extensive, this research shows that the  $T_g$  is highly dependent on the specific plasticizers and processing methods, reinforcing the need to specifically characterize the differential scanning calorimetric response of cellulose acetate found in commercially available cigarette filters.

The primary goal of the research leading to this report is to establish baseline characteristics of unsmoked cigarette filters while establishing repeatable methods that can inform future investigations on this common pollutant and its impact on the environment. In this study, we developed a systematic approach to benchmark the physicochemical properties of cellulose acetate using infrared spectroscopy (FTIR), leading to the calculation of the degree of substitution (Fei et al. 2017). The thermal response of the pristine polymer extracted from unsmoked cigarettes was characterized using differential scanning calorimetry (DSC) and thermogravimetric analysis (TGA), where the resulting thermographs and thermograms, respectively, identify the thermal transition and decomposition temperatures. To the authors' knowledge, this research constitutes the first comprehensive analysis of cellulose acetate from manufactured cigarette filters. Therefore, this study aims to fill this gap in scientific literature, creating the foundations for comprehensive environmental investigations of the short and long-term effects of littered cigarette filters.

**Fig. 1** Schematic anatomy of a typical cigarette, showing the primary components



## Materials and methods

# Sample preparation

Cigarette filters are primarily made of plasticized cellulose acetate. According to the manufacturer of Marlboro® cigarettes (Phillip Morris), the primary plasticizers include triacetin with *ca.* 10 *wt.*% and polyethylene glycol 200 with up to 8 *wt.*%. Other minor additives include titanium dioxide, aluminum oxide, and sodium chloride, adding up to < 1 *wt.*% of the filter. The cigarette filters comprise tightly tangled fibers of the plasticized cellulose acetate wrapped in and glued to the plug wrap (predominantly made of cellulose acetate). The plug is then aligned with the cigarette rod containing the tobacco, and the tipping paper secures the two together. Figure 1 shows a schematic anatomy of a typical cigarette consisting of the components mentioned above.

The unsmoked cigarette filters used in this study were obtained by removing the filters from commercially available Marlboro® Red cigarettes. The tobacco and the cigarette paper surrounding the tobacco were cut off from the rest of the cigarette at the end of the tipping paper using a stainless-steel blade. Any remaining tobacco was lightly scraped off the filter. The blade was then used to cut a slice in the plug wrap and tipping papers along the length of the cigarette filter. This slice was placed offset to the glue strip used to adhere the filter to the plug wrap and tipping papers so that the filter could quickly be unraveled and pulled away from the glue. Five filters were extracted at random from the unsmoked packs of cigarettes for each characterization regiment. Finally, pristine cellulose acetate powder (CAS 9004-35-7, Sigma-Aldrich) was used as the control in this study with a number-averaged molecular weight (M<sub>n</sub>) of ~50,000 g/mol and a degree of substitution



of 2.4–2.5 (calculated from the given acetyl wt.% of 39.2–40.2%).

# Fourier transform infrared spectroscopy (FTIR)

A section of each filter ~6 mm long was separated using a clean and sharp stainless-steel blade to obtain the spectroscopy samples. The exterior sides of the extracted filter sections were then carefully sliced off to exclude all plug wrap, tipping paper, and glue from consideration in subsequent spectroscopic analysis, resulting in cylinders with an oval cross-section. The filter sections were then pressed into thin flakes using a 12-ton hydraulic press, with the compression direction radial to the filter and normal to the sliced faces (diagram included in the Supplementary Document). Moreover, the cellulose acetate powder was similarly pressed into a disc using the hydraulic press. Infrared spectra were collected using an FTIR-ATR spectrometer (Thermo Scientific, Nicolet iS5 with the OMNIC software) using a 64-scan average and a resolution of 1 cm<sup>-1</sup>. The samples were scanned from 400 to 4000 cm<sup>-1</sup>, capturing the fingerprint and identifying groups of cellulose acetate. The peaks used to determine the DS of the cellulose acetate are around 1040 and 1240 cm<sup>-1</sup> based on the study by Fei et al. (2017). These peaks correspond to the stretching of the C-O bond in the cellulose backbone and the C-O bond in the ether in the acetyl group, respectively. Consequently, changes to the DS affect the intensities of the spectral peaks associated with the ether groups but not the backbone. The samples used to calculate the DS were intentionally left in ambient conditions, as forming the two reference baselines used in the DS spectra comparison requires a peak around 1640 cm<sup>-1</sup> caused by the bending of the bonds in absorbed water (Fei et al. 2017).

# Thermogravimetric analysis (TGA)

TGA samples were sliced using a stainless-steel blade and a newly designed and fabricated guided sectioning device (details included in the *Supplementary Document*) to ensure consistent sample size and geometry. The latter is imperative since the resulting thermograms are sensitive to the heating rate (based on the thermal properties of the materials, *e.g.*, thermal conductivity) as well as the size and geometry of the sample (affecting the

heat transfer processes occurring during pyrolysis) (Youssef 2021). All samples were between 1.6 and 1.9 mm thick and weighed ca. 9-10 mg. TGA samples were dehydrated under N<sub>2</sub> before testing for up to 20 min. The TGA testing (TA Instruments, TGA Q50) consisted of three steps. In the first step, the sample was heated to 50 °C and held isothermal at 50 °C for 2 min. The second step ramped the temperature to 750 °C at 10 °C/min. Finally, the decomposed sample was allowed to cool to room temperature under natural convection conditions. The resulting thermograms were differentiated with respect to temperature, resulting in the differential thermogravimetry curve (DTG) that represents decomposition as a function of temperature. Prominent peaks in the DTG plots are taken as the respective decomposition temperatures. In this TGA analysis, the characterization accounts for inter- and intra-filter variations. Therefore, samples were extracted from three different locations within each filter, including the mouth, middle, and tobacco sides, as depicted in Fig. 2b. At least four samples were tested from each location (mouth, middle, and tobacco sides of the cigarette filter), and the results were averaged. Statistical analyses of the decomposition temperature were performed as a function of location using a multi-way analysis of variance (ANOVA). TGA characterization of the control cellulose acetate powder faithfully followed the same procedure outlined above with two minor variations: (1) the powder was spread to ensure a complete covering of the bottom of the pan and even thickness, and (2) the average starting weight was ~13-14 mg. Additionally, the average decomposition temperatures from five samples of the cellulose acetate powder serve as reference transitions. Finally, the activation energy of the decomposition of the filters and the CA powder was determined using the procedure outlined in ASTM E1641-23 (2023). The proceeding measurements were repeated at four heating rates, varying from 5 to 20 °C/min in 5 °C/min increments. The equilibrium temperature to establish the reference loss datum was set at 300 °C, and the decomposition percentages used in the analysis ranged between 10 and 20 wt.% with an increment of 1 wt.%. Activation energies of each filter and powder sample set were taken as the average result across the decomposition percentage range.



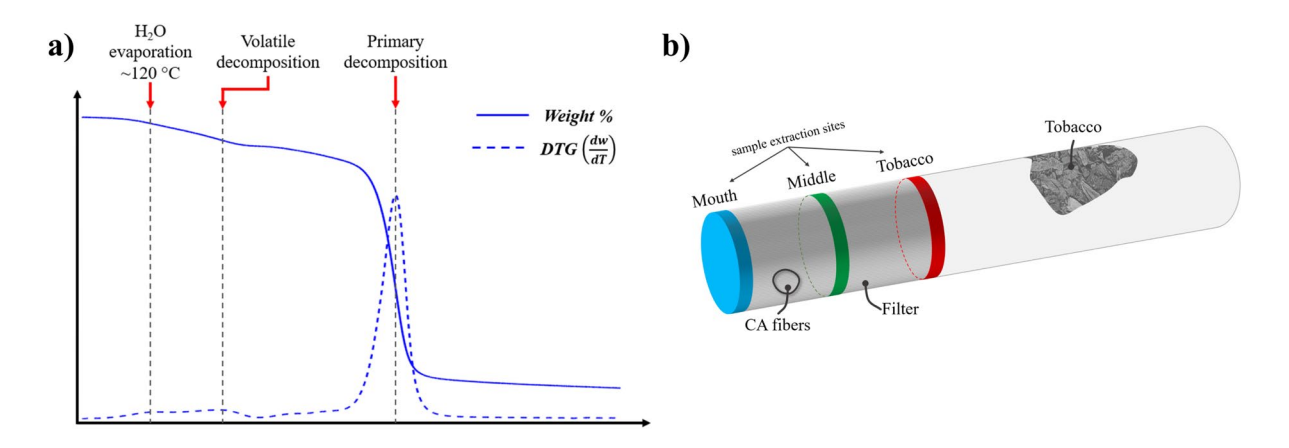


Fig. 2 a Summary of the thermogravimetric analysis, and b sample extraction sites for TGA and DSC characterization of inter- and intra-filter variation

## Differential scanning calorimetry (DSC)

DSC samples were prepared identically to the TGA counterparts using the guided sectioning method, resulting in similar 1.6-1.9 mm thick discs. The differential calorimetry testing was performed on a DSC25 (TA Instruments). The DSC samples must be packed into 5 mm diameter pans for testing; therefore, the discs were divided into two semi-circular sections. One half-disc was then carefully compressed and placed into the DSC pan (TA Tzero aluminum pans), where the filter fibers were aligned vertically along the axis of the pan. The samples were lightly tamped down to ensure consistent contact with the bottom of the pan and to eliminate stray fibers from negatively affecting the heat transfer process during testing. The packed pans were then sealed with hermetic lids (TA Tzero aluminum hermetic lids) with a 0.4 mm hole for pressure release. This scrupulous sample preparation procedure ensured a consistent mass of 3.9–4.8 mg, which is imperative for repeatable measurements, as changes in sample size and weight can drastically affect the surface areato-volume ratio and the heat flow through the sample. The DSC samples were also dehydrated under  $N_2$  for up to 20 min before the hermetic lid sealing. The test started at ambient temperature, ramped up to 325 °C, held isothermal at 325 °C for 120 s, ramped down to -50 °C, held isothermal at -50 °C for 60 s, and ramped back up to 325 °C. All heating and cooling rates were 10 °C/min. The glass transition temperature (T<sub>g</sub>) was taken from the second heat at the half-height of the transition drop (extending 50 °C into the leading and trailing plateaus) to avoid the influence of the thermal history. Inter- and intra-filter variations were accounted for using statistical analyses performed on data from samples taken from three sites (Fig. 2b) using a multi-way ANOVA as a function of location and weight. Five samples were tested from each of the mouth, middle, and tobacco sides of the cigarette filter, and the results were averaged. DSC characterization of the CA powder followed the steps discussed above, noting that the DSC pans were filled approximately halfway with the cellulose acetate powder. The powder was spread to an even thickness and lightly tamped to ensure consistent contact with the bottom. The CA powder was dehydrated under N<sub>2</sub> before the hermetic lid was sealed to the pan. The cellulose acetate powder sample weight ranged from ~8–9 mg. Five samples of the cellulose acetate powder were also tested.

# Micrographic characterization

Optical microscopy (OM) was performed using a Keyence VHX-7100 digital microscope. Lighting conditions were adjusted based on the sample geometry and reflectiveness to ensure image clarity. Composite images were acquired by imaging at differing focal planes to represent the depth of the fibers comprehensively. Additionally, scanning electron microscopy (SEM) was performed on a Quanta 450 at a high vacuum with accelerating voltage ranging between 2 and 20 kV and working distances of 10 to 15 mm.



All SEM samples were platinum sputter coated to a thickness of 6 nm using a Q150T (Quorum Technologies EMS). Conductive double-sided carbon tape was placed along the sides of the filter samples to help prevent charging on individual ungrounded fibers. Finally, the cellulose acetate powder was also imaged using the SEM to ascertain the difference in the topology and morphology.

## Results and discussion

# Physicochemical properties

Figure 3 shows the infrared spectra of CA fibers extracted from unsmoked cigarette filters and the control pristine CA powder using FTIR-ATR between 400 and 4000 cm<sup>-1</sup> to ascertain their chemical composition and structure. Table 1 summarizes the respective spectra peaks and the associated bond

vibration, affirming the presence of the characteristic peaks of cellulose acetate, as previously reported by Dias et al. (1998), Ilharco and Barros (2000), Murphy and Pinho (1995), and Oldani and Schock (1989). Specifically, the primary spectral peaks at 1734, 1367, 1215, and 1031 cm<sup>-1</sup>, corresponding to stretching of the C=O double-bond ( $\nu_{C=O}$ ) in the carbonyl group, stretching of -OH ( $\nu_{OH}$ ) in the cellulose backbone and the unacetylated hydroxyl groups, stretching of C-O ( $\nu_{CO}$ ) in the ether group, and stretching of the C-O-C bonds ( $\nu_{\text{C-O-C}}$ ) in the pyranose rings are in excellent agreement with referenced literature (Dias et al. 1998; Ilharco and Barros 2000; Murphy and Pinho 1995; Oldani and Schock 1989). In the functional group region, the broad peaks around 3500 cm<sup>-1</sup> ( $\nu_{OH}$  in the hydroxyl group) and the peaks at 2880 and 2942 cm<sup>-1</sup> ( $\nu_{CH}$  in the acetyl group) also closely match those reported a priori (Dias et al. 1998; Ilharco and Barros 2000; Oldani and Schock 1989). While it is imperative

Fig. 3 FTIR spectra of CA fibers extracted from unsmoked cigarette filters compared to the spectra of unprocessed CA powder

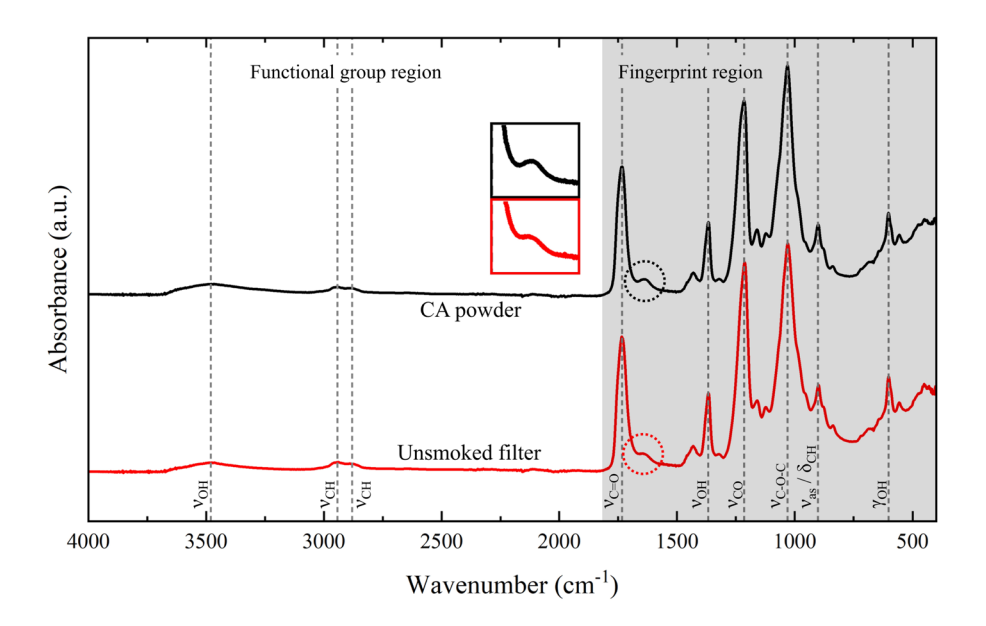


**Table 1** FTIR spectral peaks of CA fibers (denoted *f*CA) extracted from unsmoked cigarette filters and pristine CA powder (control demarked as *p*CA)

Wavenumber (cm <sup>-1</sup> )	Functional groups (Ilharco and Barros 2000)
1734 (fCA and pCA)	$\nu_{C=O}$ in the carbonyl group
1366 (fCA) & 1367 (pCA)	$\nu_{OH}$ in the backbone and hydroxyl groups
1213 (fCA) & 1215 (pCA)	$\nu_{\mathrm{CO}}$ in the ether group
1030 (fCA) &1031 (pCA)	$\nu_{\text{C-O-C}}$ in the pyranose ring
899 (fCA) & 901 (pCA)	$\nu_{as}$ in the pyranose ring or $\delta_{CH}$ out of plane
601 (fCA) & 602 (pCA)	$\gamma_{OH}$ out of plane



to reiterate that changes in spectral intensity are directly mapped to the morphology of the samples and scanning conditions (note that the applied pressure was always regulated by the instrument), such spectral variance might be attributed to the plasticizers and other chemical additives used to facilitate the manufacture and utility of the cigarette filters (e.g., fire retarding agents). The changes in spectral intensity are specifically prominent within the fingerprint region of the FTIR results plotted in Fig. 3. However, the lack of stereoregular structure of the CA backbone prohibits further speculation about the underlying molecular sources of changes in the spectral intensities. One notable difference between the two spectra is the decrease in the intensity of the water-induced shoulder at 1636 cm<sup>-1</sup> (corresponding to H-O-H bending (Fei et al. 2017)) in the unsmoked filter spectra compared to the CA powder (shown in the inset in Fig. 3), illustrating the difference in water absorption between fibers and powder.

The degree of hydroxyl group substitution (DS) in the cellulose acetate structure was calculated using the FTIR spectra in Fig. 3 using the methods described by Fei et al. (2017) based on

$$DS = 1.8742 - 1.2541r + 1.9760r^2 \tag{1}$$

where r is the relative intensity of the 1213 cm<sup>-1</sup> peak with respect to the 1030 cm<sup>-1</sup> peak. The peak intensity at 1213 cm<sup>-1</sup> was deduced upon defining the baseline between the valleys located at 935 and 1580 cm<sup>-1</sup>. The DS for CA fibers from unsmoked cigarette filters and control powder are 2.53 and 2.28, respectively. Notably, the calculated DS for the CA powder is slightly lower than the specifications provided by the manufacturer (DS  $\approx 2.4-2.5$ ), which is attributed to the broad variance in the powder morphology and light-cellulose interactions during FTIR measurements. In general, differences between the values reported herein and those provided elsewhere are associated with the elimination of all post-processing steps, i.e., CA powder was characterized as received. The authors opted for this approach to avoid (1) alteration of the cellulose chemical structure to provide a reasonable assessment of the reference material and (2) changes to the CA fibers extracted from the filters to emulate the conditions upon disposal closely. On the other hand, the DS of the cellulose acetate fibers extracted from off-the-shelf cigarette filters is consistent with the general characteristics of CA while providing the first quantitative attribute of the processed CA fibers, to the best knowledge of the authors. The higher DS value for the CA fibers from the unsmoked cigarettes suggests reduced biodegradability (Buchanan et al. 1996; Kim et al. 2023; Puls et al. 2011), resulting in longer persistence in nature after disposal.

Optical and electron microscopy analyses accompanied the spectroscopic measurements listed above to further accentuate the irregular morphology of cellulose acetate fibers and powders studied herein. Figure 4 is a collage of optical micrographs of the CA fibers extracted from the cigarette filters (Fig. 4a) and the control CA powder (Fig. 4b), while Fig. 5 comprises the respective SEM micrographs. Figure 4a is an optical micrograph of the CA fibers extracted from the unsmoked filter, elucidating the fiber entanglements with 100s of fibers within the  $\sim 1$  mm  $\times 1$  mm observation area and the optical transparency at the fiber level. The fiber entanglements within the cigarette filter provide small porosity to stop unsmoked tobacco particles and ash during puffing and inhalation and give structural consistency for handling and smoking. The composition of the filters with single fibers that are externally plasticized (softening agents to bind fiber tows together) is conducive for high throughput manufacturing and assembly. Despite the predominate transparency, the single fiber morphology also indicates the presence of randomly distributed white speckles  $(\mathcal{O}(1\mu m))$ , evidencing chemical additives (e.g., added carbon for additional filtration) and residues from the manufacturing steps. Image processing of optical micrographs in Fig. 4a indicates the fiber width is ~30 µm with a large standard deviation (up to 30%) for inter- and intra-fiber measurements based on size changes due to the malleable nature of CA and the fiber cross-sectional geometry. Figure 4b is an optical micrograph of the CA powder with an average particle size of  $\mathcal{O}(10-100\mu m)$ and irregular morphology. The latter contributes to the lack of comparable transparency to that shown in Fig. 4a. In general, the structural and surface morphologies contribute to the variation in the spectroscopic data, as discussed above.

Figure 5a comprises SEM micrographs of an unsmoked cigarette filter and a higher magnification of the cross-section of an individual CA fiber. The latter has an apodictically trilobal cross-sectional



Fig. 4 Optical micrographs of a an unsmoked cigarette filter with a closeup of an isolated fiber and b CA powder with a closeup of an individual particle

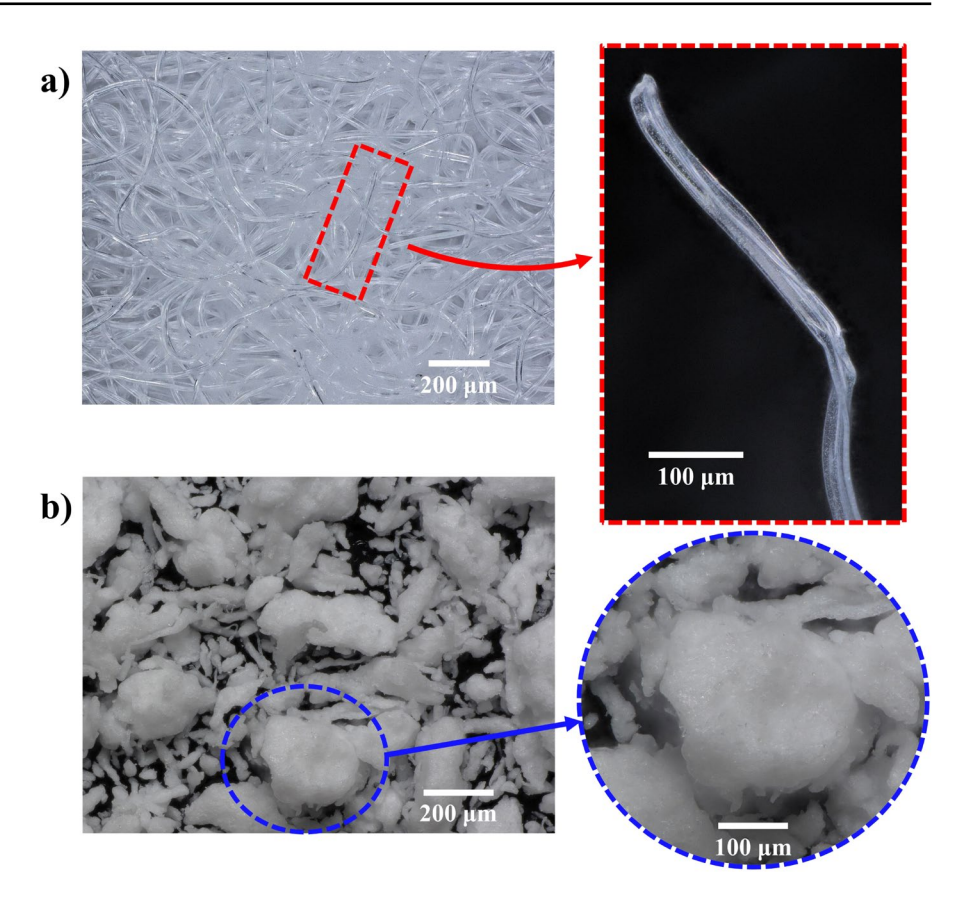
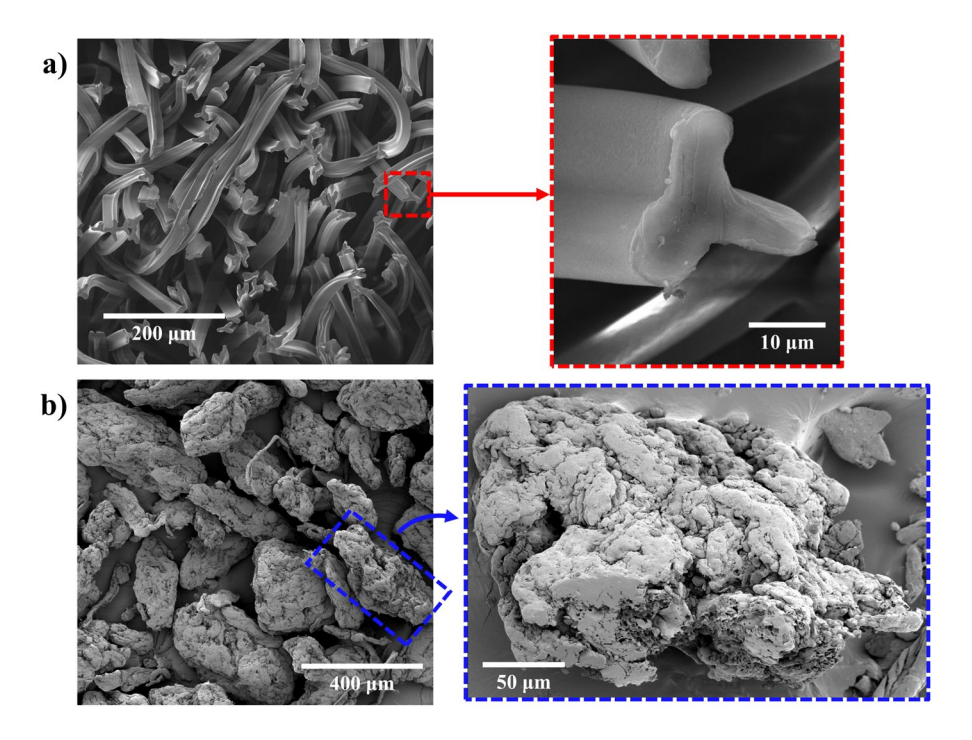


Fig. 5 Scanning electron (SEM) micrographs of a CA fibers extracted from an unsmoked cigarette with a higher magnification micrograph of the trilobal fibers, and b CA powder





geometry to increase the surface-to-volume ratio. Moreover, the morphology of the CA fibers is also responsible for the sheen depicted in Fig. 4a. Increasing the surface area (with respect to the overall filter volume) improves the filtration efficacy as part of the filter functionality during smoking, enhances the structural stability of the filter by promoting more entanglement, and assists in heat transfer or surface degradation after disposal (Puls et al. 2011). The shininess of the fibers (Fig. 4a) ascertain the conclusions above about the externally applied additives. Finally, Fig. 5b encompasses SEM micrographs of CA powders at two magnification levels, showing their irregular morphology.

## Thermal decomposition properties

Figure 6a represents a typical thermogram of CA fibers extracted from unsmoked cigarette filters and control CA powder as a function of temperature, ranging from 50 to 750 °C, elucidating thermal decomposition. Notably, the thermograms in Fig. 6a are the average of at least five separate measurements from each of the considered materials. Figure 6b shows the differential thermogravimetric (DTG) behavior of the studied materials, axiomatically epitomizing the decomposition transitions. While the weight of the benchmark CA powder remained nearly unchanged up to the onset of decomposition at 300 °C, the CA fibers from the cigarette filters exemplified a distinct progressive pyrolysis up to 230 °C. The latter transpired in the DTG plot, with two preceding peaks at

125 and 190 °C attributed to the moisture evaporation within the intertwined fibers (Fig. 6) and the release of low-temperature volatiles and residues from the chemical treatment and manufacturing processes. However, the primary decomposition temperatures of the unsmoked filter fibers and CA powder (coinciding with the location of the prominent peak in the DTG plot) are 370.1  $\pm$  0.8 and 375.8  $\pm$  0.9 °C, respectively. The primary decomposition temperatures agree with that reported by Quintana et al. (2013) (ca. 372 °C) and others (Candido et al. 2017; Meireles et al. 2007; Teixeira et al. 2021, 2023). The dichotomy between the pyrolysis of CA fibers from the cigarettes and pristine CA powder affirms the influence of processing conditions on the thermal stability of the polymer, evidencing potential unique decomposition behavior in nature due to the reactivity of the additives with the surrounding environment (e.g., moisture retention in the fibers). In other words, the distinct pyrolysis implies that H<sub>2</sub>O/CA fiber interactions might result in leachate release into the soil and water column, a topic of future research by this group.

At this junction, an important question persisted: Does the sample extraction site make a difference in the decomposition behavior of CA fibers? Hence, CA fibers were extracted from three regions within the unsmoked cigarette filters, as shown in Fig. 2b. The extracted samples underwent identical pyrolysis faithful to the conditions described in the TGA methods section, focusing on the primary decomposition temperature. The results in Fig. 7b accentuate the insensitivity of thermal composition and stability of the CA

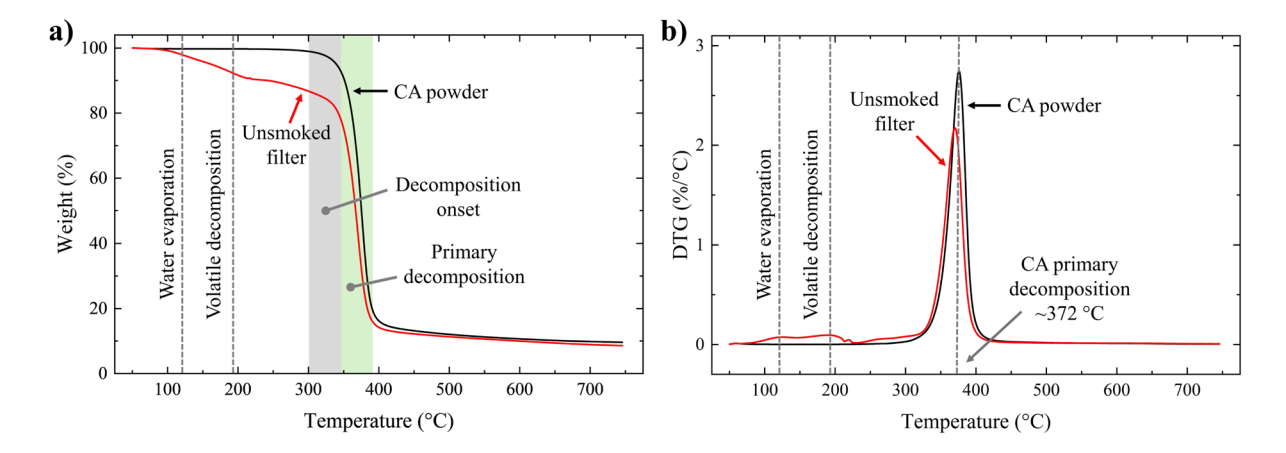
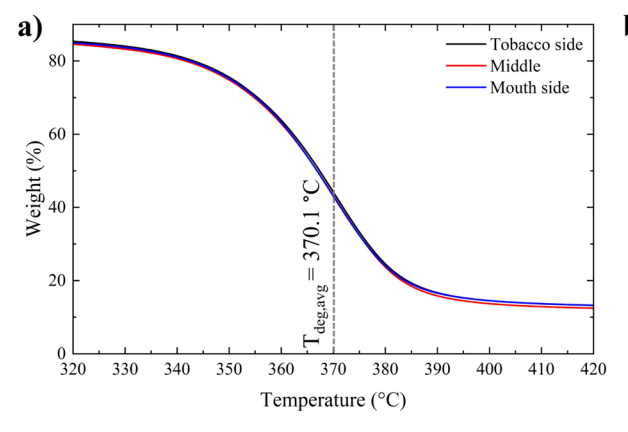
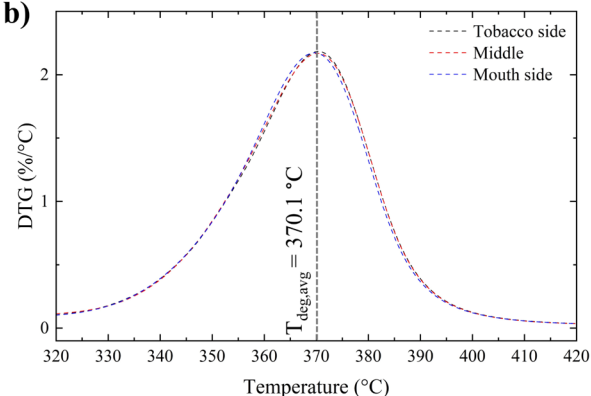


Fig. 6 a Pyrolysis of CA powder and CA fibers extracted from the unsmoked cigarette filters (average thermograms) and b Differential thermogram (DTG) plot of CA powder and CA fibers from cigarette filters (average DTGs)







**Fig. 7** a Pyrolysis of CA fibers (average thermograms), and **b** differential thermogram plot of CA fibers (average DTGs) from cigarette filters around the primary decomposition peak

(370.1 °C) as a function of extraction sites (*e.g.*, mouth, middle, and tobacco sides), epitomizing insensitivity to the location on the filter

fibers to the extraction location. The primary degradation temperatures were  $369.7 \pm 1.1$ ,  $370.3 \pm 0.4$ , and 370.4  $\pm$  0.2 °C for samples extracted from the mouth, middle, and tobacco sides, respectively. Furthermore, statistical analysis using ANOVA affirmed the insensitivity conclusion as a function of the extraction location from the unsmoked filters, reporting a p-value of 0.32, i.e., a statistically insignificant difference at a 95% confidence interval. The residue weight percentage was also recorded and analyzed to see if there was a difference in the remains at the end of the test. A final confirmation of the nearly identical pyrolysis of CA fiber despite the variation in the extraction site transpired from comparing the average residues,  $8.0 \pm 0.8$ ,  $8.7 \pm 0.8$ , and  $9.2 \pm 0.1\%$ , respectively. Similarly, ANOVA indicated statistical insignificance with a p-value of 0.37 for the weight residues at the same confidence interval. That is to say, the thermal decomposition of unsmoked cigarette filters is invariant to the processing conditions (i.e., inter-filter invariability) and extraction location (i.e., intra-filter consistency).

The utility of thermogravimetric analysis is extended to determine the activation energy of the CA fibers extracted from the unsmoked cigarette filters and the benchmarking CA powder by performing pyrolysis at different heating rates (5, 10, 15, and 20 °C/min). The activation energy calculations were done in accordance with the Flynn-Wall-Ozawa method of kinetic decomposition analysis cataloged in ASTM E1641-23 (2023). The premise

of kinetic decomposition analysis hinges on accelerating the pyrolysis as a function of the heating rate. An increase in the latter is associated with a relatively delayed decomposition since pyrolysis is governed by convection and conduction heat transfer modes. Five sample sets from CA fibers and powder were characterized using the TGA at each of the above heating rates. Figure 8 plots the heating rates as a function of inverse decomposition temperatures for CA fibers (Fig. 8a) and powder (Fig. 8b) at 10, 15, and 20% conversion levels, where the activation energy is linearly correlated to the slope of the fit line. The average activation energy for the CA fibers extracted from the unsmoked cigarettes is  $184.3 \pm 7.6 \text{ kJ/mol}$ , whereas the CA powder has an activation energy of  $185.0 \pm 9.9$  kJ/mol. The slight variance in the activation energies of the CA fibers is attributed primarily to the stabilizing additive chemicals, which potentially also affect the natural decomposition after disposal (beyond the focus of this research but of great interest to this group for future endeavors). The close agreement between the activation energies of CA fibers and powder suggests the analysis method used herein converged well on identifying the characteristics of cellulose acetate.

# Thermal transitions

Figure 9a shows typical DSC thermographs from thermal testing CA fibers (extracted from three sites as shown in Fig. 2b) and CA powder as a function



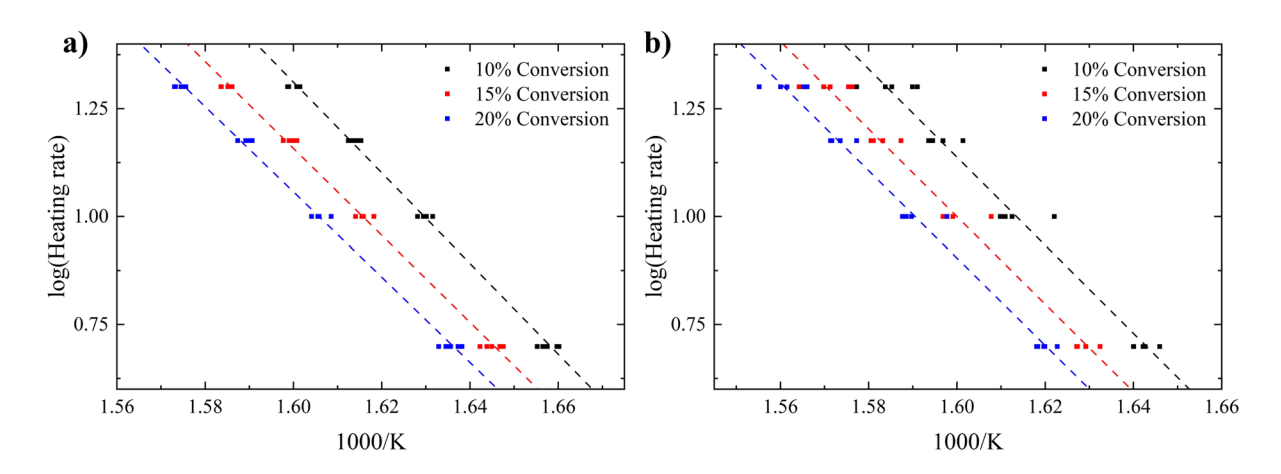


Fig. 8 Arrhenius plot of the natural log of the heating rate vs inverse decomposition temperature at constant conversions for a unsmoked cigarette filters and b CA powder

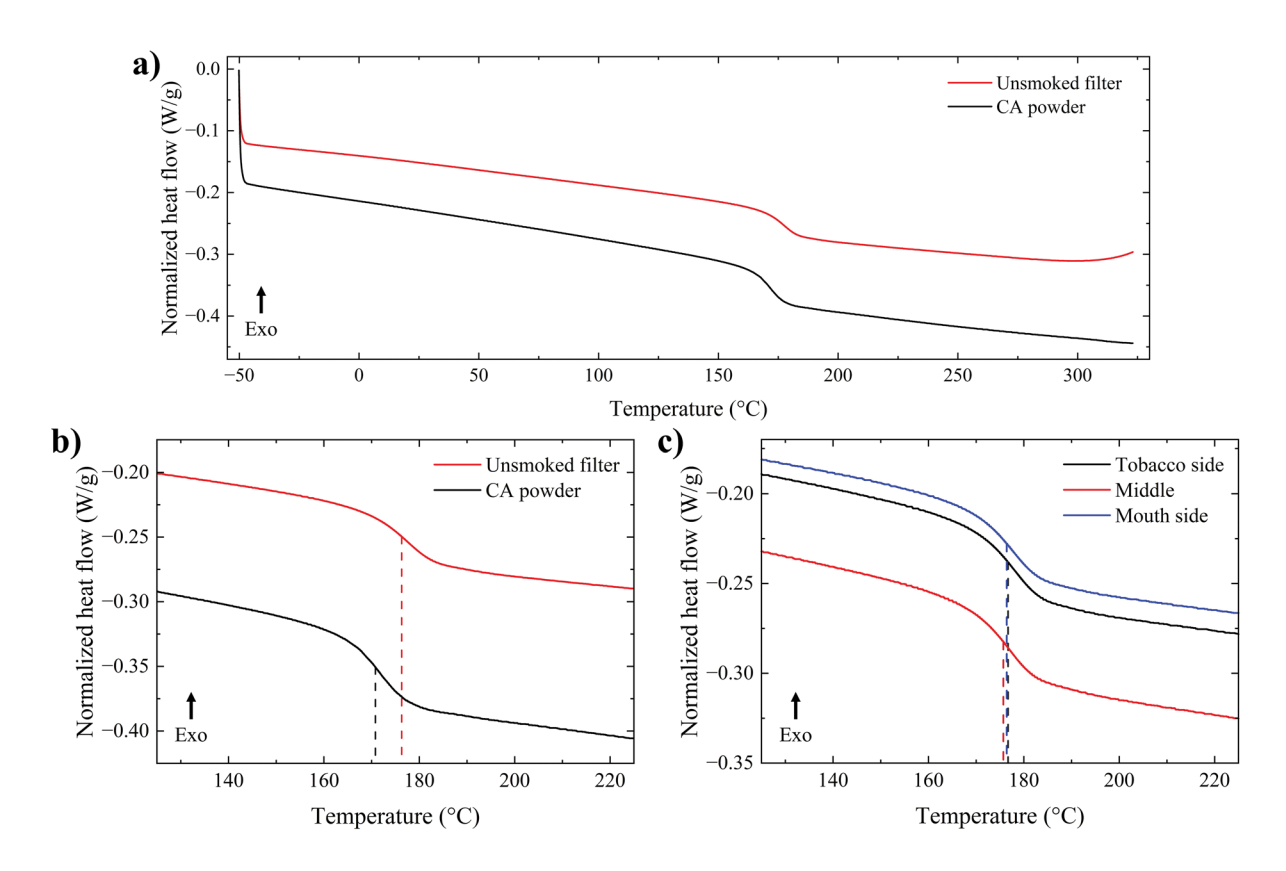


Fig. 9 a Typical DSC thermographs of CA fibers and powder,  $\mathbf{b}$  the respective heat flux around glass transition, and  $\mathbf{c}$  the effect of extraction site on the glass transition of fibers extracted from unsmoked filters

of temperature ranging from -50 to 325 °C at a rate of 10 °C/min, as discussed in the DSC methods section. It is imperative to reiterate that all analyses were done based on the second heating cycle

to minimize the effect of thermal history from any pre-testing conditions (*e.g.*, manufacturing parameters, volatiles, and low-temperature additives).



The thermographs in Fig. 9a elucidate three crucial experimental observations. First, the endothermic drop associated with the glassy transition (denoted in Fig. 9b), being a progressive transition, points to the amorphous macromolecular structure of cellulose acetate lacking short- and long-range order (Kalogeras and Hagg Lobland 2012). The high entropy associated with amorphous polymers reduces the heat (plotted on the ordinate of the thermographs in Fig. 9) to liberate the chain mobility into the rubbery regime and beyond. Second is that the average  $T_g \approx 176.3 \pm 0.7$  °C for CA fibers extracted from the unsmoked cigarette filters is higher than the average  $T_g \approx 170.8 \pm 1.7$  °C for control CA powder. This increase in the glass transition of the CA fibers compared to the powder counterpart contradicts the Flory-Fox equation predictions, implying the addition of plasticizers (as in CA fibers) is associated with lower T<sub>g</sub> (Fox and Flory 1950). The relatively high glass transition of the CA fibers is attributed to (1) the distinct difference in the morphology between the trilobal fibers and irregular CA powder (Fig. 5), (2) the increase in the inter-fiber free volume due to the entanglement (Fig. 5), and (3) the external addition of plasticizers to promote bonding and structural stability (Fig. 4). Nonetheless, the measured glass transition temperature can be used to estimate the melting temperature of this amorphous polymer, irrespective of the morphology, e.g., fibers and powder, such that  $T_m \approx 1.55T_g$  (Lee and Knight 1970), resulting in  $262^{\circ}\text{C} < T_m < 272^{\circ}\text{C}$ , consistent with the reported melting temperature of cellulose acetate (Kamide and Saito 1985; Patel et al. 1970). Finally, the glass transition of the CA fibers extracted from the unsmoked cigarette filters is insensitive to the extraction sites (Fig. 2b). Figure 9c shows the thermographs of CA fibers extracted from mouth side, middle, and tobacco side sites, resulting in average glass transition temperatures of 176.7  $\pm$  0.6, 175.7  $\pm$  0.5, and 176.4  $\pm$  0.7 °C, respectively. The insensitivity of the glass transition to the extraction site is confirmed by ANOVA with a p-value = 0.13, indicating statistical insignificance at a 95% confidence level. In general, the thermal behavior of CA fibers and powder from the TGA and DSC suggests that further characterization can be based on randomized samples extracted from arbitrary locations of the filters.

#### Conclusion

Cellulose acetate is a ubiquitous polymer in several applications, the prime of which is cigarette filters. Littered filters are considered prolific pollutants, potentially impacting waterways and marine life. This research investigated the physicochemical and thermal properties of cellulose acetate extracted from unsmoked cigarette filters and benchmarked the attributes to those measured from pristine CA powder. A comprehensive characterization regiment leveraged spectroscopic, microscopic, thermogravimetric, and calorimetric approaches. The primary outcomes of this research are based on an investigation of CA fibers specifically extracted from Marlboro® Red cigarettes (laying the foundation for future research to encompass the effect of the manufacturing processes used by different brands), leading to four major conclusions. First, FTIR analysis affirmed the molecular structure of cellulose acetate in CA fibers and powder by identifying the characteristic spectral peaks in the functional group and fingerprint regions, which led to the degree of substitution (DS) calculation. Higher DS suggests reduced biodegradability upon disposal of CA-based cigarette filters. Second, the pyrolysis of CA fibers extracted from unsmoked cigarettes affirmed their affinity to atmospheric moisture and the presence of volatiles preceding the primary decomposition of cellulose acetate. The degradation behavior is insensitive to inter- and intra-filter variabilities. Third, the thermal transitions of cellulose acetate, irrespective of the source, were measured using differential scanning calorimetry. Changes in glass transition were correlated to morphology, fiber entanglements or powder agglomeration, and additives used in cigarette filter processing. Finally, analysis of variance statistical testing confirmed that the effect of the extraction site is statistically insignificant, allowing for the generalization of the filter characterization irrespective of the sample extraction location. The outcomes of this research introduce the first scientific investigation to benchmark the physicochemical and thermal properties of cellulose acetate extracted from cigarette filters, assisting in demystifying their resiliency in the environment upon disposal.



Author contributions E.W.: Methodology, Validation, Formal Analysis, Investigation, Data Curation, Writing—Original Draft, Writing—Review & Editing, Visualization. M.S.: Methodology, Resources, Writing—Review & Editing, Project Administration. E.H.: Conceptualization, Methodology, Resources, Writing—Review & Editing, Supervision, Project administration, Funding acquisition. S.P.: Methodology, Writing—Review & Editing. N.M.: Conceptualization, Methodology, Resources, Writing—Review & Editing, Supervision, Funding acquisition. G.Y.: Conceptualization, Methodology, Validation, Formal analysis, Investigation, Resources, Writing—Original Draft, Writing—Review & Editing, Visualization, Supervision, Funding acquisition.

**Funding** This material is based upon work supported by funding from the Tobacco-Related Disease Research Program (T33IR6723). The authors are also grateful for internal funding from San Diego State University. The research leading to these results was partly supported by the United States Department of Defense under Grant Agreement Nos. W911NF1410039, W911NF1810477, W911NF2210199, W911NF2310150, W911NF2310329, N00014-22-1-2376 and N00174-23-1-0009, and by the National Science Foundation grants CMMI-1925539 and CMMI-2035663. The authors also acknowledge the use of equipment at SDSU's Electron Microscopy Facility acquired by NSF grant DBI-0959908.

**Data availability** The data that support the findings of this study are available from the corresponding author, G.Y., upon reasonable request.

## **Declarations**

**Conflict of interest** The authors declare no competing interests.

Ethical approval Not Applicable.

#### References

- ASTM (2023) ASTM E1641: standard test method for decomposition kinetics by thermogravimetry using the Ozawa/ Flynn/wall method. ASTM International, West Conshohocken, PA
- Bao CY, Long DR, Vergelati C (2015) Miscibility and dynamical properties of cellulose acetate/plasticizer systems. Carbohydr Polym 116:95–102. https://doi.org/10.1016/j.carbp ol.2014.07.078
- Buchanan CM, Dorschel D, Gardner RM, Komarek RJ, Matosky AJ, White AW, Wood MD (1996) The influence of degree of substitution on blend miscibility and biodegradation of cellulose acetate blends. J Environ Polym Degrad 4(3):179–195
- Candido RG, Godoy GG, Gonçalves AR (2017) Characterization and application of cellulose acetate synthesized from sugarcane bagasse. Carbohydr Polym 167:280–289. https://doi.org/10.1016/j.carbpol.2017.03.057

- Charvet A, Vergelati C, Long DR (2019) Mechanical and ultimate properties of injection molded cellulose acetate/plasticizer materials. Carbohydr Polym 204:182–189. https://doi.org/10.1016/j.carbpol.2018.10.013
- de Lucena MdCC V, Alencar AE, Mazzeto SE, Soares SA (2003) The effect of additives on the thermal degradation of cellulose acetate. Polym Degrad Stab 80(1):149–155. https://doi.org/10.1016/S0141-3910(02)00396-8
- Dias CR, Rosa MJ, de Pinho MN (1998) Structure of water in asymmetric cellulose ester membranes and ATR-FTIR study. J Membr Sci 138(2):259–267. https://doi.org/10.1016/S0376-7388(97)00226-3
- Erdmann R, Kabasci S, Heim HP (2021) Thermal properties of plasticized cellulose acetate and its beta-relaxation phenomenon. Polym (Basel) 13(9):1356
- Fei P, Liao L, Cheng B, Song J (2017) Quantitative analysis of cellulose acetate with a high degree of substitution by FTIR and its application. Anal Methods 9(43):6194–6201. https://doi.org/10.1039/c7ay02165h
- Ferreira GM, Herdi DdS, Da Silveira KC, Gonçalves MC, Andrade MC (2022) Evaluation of thermal degradation kinetics of hybrid cellulose acetate membranes using isoconversional methods. VETOR - Rev Ciênc Exatas Eng 32(1):52–61
- Filho GR, Monteiro DS, Meireles CdS, de Assunção RMN, Cerqueira DA, Barud HS, Ribeiro SJL, Messadeq Y (2008) Synthesis and characterization of cellulose acetate produced from recycled newspaper. Carbohydr Polym 73(1):74–82. https://doi.org/10.1016/j.carbpol.2007.11.
- Fischer S, Thümmler K, Volkert B, Hettrich K, Schmidt I, Fischer K (2008) Properties and applications of cellulose acetate. Macromol Symp 262(1):89–96. https://doi.org/10.1002/masy.200850210
- Flynn JH, Wall LA (1966) A quick, direct method for the determination of activation energy from thermogravimetric data. J Polym Sci B Polym Lett 4(5):323–328. https://doi.org/10.1002/pol.1966.110040504
- Fox TG Jr, Flory PJ (1950) Second-order transition temperatures and related properties of polystyrene. I. influence of molecular weight. J Appl Phys 21(6):581–591. https://doi.org/10.1063/1.1699711
- Gola D, Kumar Tyagi P, Arya A, Chauhan N, Agarwal M, Singh SK, Gola S (2021) The impact of microplastics on marine environment: a review. Environ Nanotechnol Monit Manag 16:100552. https://doi.org/10.1016/j.enmm. 2021.100552
- Ilharco LM, Brito de Barros R (2000) Aggregation of pseudoisocyanine iodide in cellulose acetate films: structural characterization by FTIR. Lagnmuir 16:9331–9337. https://doi.org/10.1021/la000579e
- Kalogeras IM, Hagg Lobland HE (2012) The nature of the glassy state: structure and glass transitions. J Mater Educ 34(3):69–94
- Kamide K, Saito M (1985) Thermal analysis of cellulose acetate solids with total degrees of substitution of 0.49, 1.75, 2.46, and 2.92. Polym J 17(8):919–928. https://doi.org/10.1295/polymj.17.919
- Kim JR, Thelusmond J-R, Albright VC, Chai Y (2023) Exploring structure-activity relationships for polymer biodegradability by microorganisms. Sci Total Environ



- 890:164338. https://doi.org/10.1016/j.scitotenv.2023.
- Lee WA, Knight GJ (1970) Ratio of the glass transition temperature to the melting point in polymers. Br Polym J 2(1):73–80. https://doi.org/10.1002/pi.4980020112
- Meireles CdS, Filho GR, de Assunção RMN, Zeni M, Mello K (2007) Blend compatibility of waste materials—cellulose acetate (from sugarcane bagasse) with polystyrene (from plastic cups): diffusion of water, FTIR, DSC, TGA, and SEM study. J Appl Polym Sci 104(2):909–914. https://doi.org/10.1002/app.25801
- Murphy D, Norberta de Pinho M (1995) An ATR-FTIR study of water in cellulose acetate membranes prepared by phase inversion. J Membr Sci 106(3):245–257. https://doi.org/10.1016/0376-7388(95)00089-U
- Oldani M, Schock G (1989) Characterization of ultrafiltration membranes by infrared spectroscopy, esca, and contact angle measurements. J Membr Sci 43(2):243–258. https://doi.org/10.1016/S0376-7388(00)85101-7
- Ozawa T (2006) A new method of analyzing thermogravimetric data. Bull Chem Soc Jpn 38(11):1881–1886. https://doi.org/10.1246/bcsj.38.1881
- Patel KS, Patel KC, Patel RD (1970) Study on the pyrolysis of cellulose and its derivatives. Makromol Chem 132(1):7– 22. https://doi.org/10.1002/macp.1970.021320102
- Puls J, Wilson SA, Hölter D (2011) Degradation of cellulose acetate-based materials: a review. J Polym Environ 19(1):152–165. https://doi.org/10.1007/s10924-010-0258-0
- Quintana R, Persenaire O, Lemmouchi Y, Sampson J, Martin S, Bonnaud L, Dubois P (2013) Enhancement of cellulose acetate degradation under accelerated weathering by plasticization with eco-friendly plasticizers. Polym Degrad Stab 98(9):1556–1562. https://doi.org/10.1016/j.polymdegradstab.2013.06.032
- Serbruyns L, Van de Perre D, Hölter D (2023) Biodegradability of cellulose diacetate in aqueous environments. J Polym Environ 32(3):1326–1341. https://doi.org/10.1007/s10924-023-03038-y
- Skornyakov IV, Komar VP (1998) IR spectra and the structure of plasticized cellulose acetate films. J Appl Spectrosc 65(6):911–918. https://doi.org/10.1007/BF02675748
- Teixeira SC, Silva RRA, de Oliveira TV, Stringheta PC, Pinto MRMR, Soares NdFF (2021) Glycerol and triethyl citrate plasticizer effects on molecular, thermal, mechanical, and

- barrier properties of cellulose acetate films. Food Biosci. https://doi.org/10.1016/j.fbio.2021.101202
- Teixeira SC, de Oliveira TV, Fortes-Da-Silva P, Raymundo-Pereira PA, Ribeiro ARC, Batista LF, Gomes NO, Stringheta PC, de Soares NFF (2023) Investigation of the influence of plasticizers on the biodegradability of cellulose acetate. J Appl Polym Sci. https://doi.org/10.1002/app. 54316
- Toprak C, Agar JN, Falk M (1979) State of water in cellulose acetate membranes. J Chem Soc Faraday Trans 1 Phys Chem Condens Phases 75:803–815. https://doi.org/10.1039/F19797500803
- Vanapalli KR, Sharma HB, Anand S, Ranjan VP, Singh H, Dubey BK, Mohanty B (2023) Cigarettes butt littering: the story of the world's most littered item from the perspective of pollution, remedial actions, and policy measures. J Hazard Mater 453:131387. https://doi.org/10. 1016/j.jhazmat.2023.131387
- Vinodhini PA, Sangeetha K, Thandapani G, Sudha PN, Jayachandran V, Sukumaran A (2017) FTIR, XRD and DSC studies of nanochitosan, cellulose acetate and polyethylene glycol blend ultrafiltration membranes. Int J Biol Macromol 104:1721–1729. https://doi.org/10.1016/j.ijbiomac.2017.03.122
- Wang B, Chen J, Peng H, Gai J, Kang J, Cao Y (2016) Investigation on changes in the miscibility, morphology, rheology and mechanical behavior of melt processed cellulose acetate through adding polyethylene glycol as a plasticizer. J Macromol Sci B 55(9):894–907. https://doi.org/10.1080/00222348.2016.1217185
- Youssef G (2021) Applied mechanics of polymers: properties processing and behavior. Elsevier, Amsterdam, Netherlands

**Publisher's Note** Springer Nature remains neutral with regard to jurisdictional claims in published maps and institutional affiliations.

Springer Nature or its licensor (e.g. a society or other partner) holds exclusive rights to this article under a publishing agreement with the author(s) or other rightsholder(s); author self-archiving of the accepted manuscript version of this article is solely governed by the terms of such publishing agreement and applicable law.

